

Maria STRAKOWSKA, Bogusław WIĘCEK
 LODZ UNIVERSITY OF TECHNOLOGY, INSTITUTE OF ELECTRONICS,
 Wólczajska 211/215, 90 924 Łódź, Poland

Thermal modeling of planar and cylindrical biomedical multilayers structures in frequency domain

Abstract

Planar and cylindrical thermal models of biomedical multilayer structures with perfusion are presented in this paper. For each layer the models are solved analytically in frequency domain using the Laplace transform. Modeling the multilayer structure allows formulating the set of linear equations with unknown integral constants. As a result, the thermal impedance $Z_{th}(j\omega)$ is calculated. Next, the poles of thermal impedance are estimated using *Vector Fitting* (VF) method. Finally, distribution of thermal time constants allows evaluating the temperature response $T(t)$ of the modeled structure.

Keywords: Thermal models, Vector Fitting, perfusion, Pennes model, Foster network.

Symbols:

k_i – thermal conductivity of i -th layer (W/m·K)
 $c_{vi} = \rho_i c_{pi}$ – specific heat (J/m³K)
 q_{vi} – dissipated power density (W/m³)
 q_{vpi} – dissipated power density including perfusion (W/m³)
 q_i – heat flux at the interface between layers (W/m²)
 j – the imaginary unit
 $\omega = 2\pi f$ – angular frequency (rad/s, f in Hz)
 L_i – diffusion length of i -th layer (m)
 w_i – perfusion coefficient (1/s)
 c_{vb} – thermal capacity of blood per volume unit (J/m³K)
 h – heat transfer coefficient (W/m²K)
 A_i, B_i – integration constants
 I_0, K_0 – modified Bessel functions of first and second kind (zero order)
 T_b – temperature of blood (K)
 CAD – Computer Aided Design
 FEM – Finite Element Method

1. Introduction

Nowadays, there are CAD tools available with implemented numerical multidimensional FEM for thermal modeling of complex multilayer objects [1-3]. Depending on the model's complexity and time resolution, such modeling requires long simulation time to get the satisfactory results. In addition, they do not implement perfusion and thermal impedance in frequency domain directly.

Actually, there is a need of tools for thermal characterization of multilayer objects, in medicine, in electronics and other fields of applications [4-9]. There are different methods of multilayer thermal object identification [10-17]. There is a system commercially available for thermal characterization of multilayer structures in electronics [18].

The problem of thermal characterization of multilayer structures is an inverse heat transfer problem, which is in general case very ill-conditioned one. In order to validate such thermal characterization of a measured multilayer structure, we first propose to perform similar characterization by modeling. One of the possible approaches is a simplified thermal modeling in frequency domain, using analytical solutions of partial differential equation for each layer [6, 8, 9]. Relatively short execution time of such modeling in contrast to 3D FEM simulations using general-purpose CAD packages is an important advantage.

2. Planar n -layer thermal model with perfusion

The presented model (Fig. 1) consists of n -planar layers with different thermal parameters and power dissipated q_{vi} . Convective heat exchange (h_0, h_n) or constant temperature boundary conditions can be defined at front and bottom surfaces. Perfusion defined by Pennes model is included as well [6, 8, 9]. Geometry of samples is in form of stacked parallel layers of thickness d_i . It corresponds to the practical medical diagnosis known as the cold stress using relatively large cooling device and measuring temperature in the middle of a cold spot. In addition, the arbitrary heat fluxes q_i can be defined at any interface between the layers – Fig. 1.

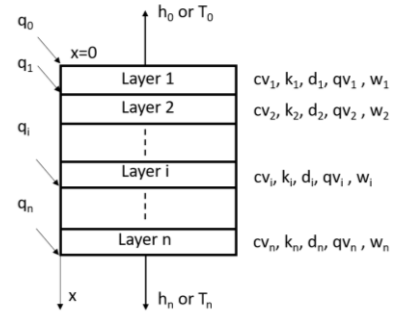


Fig. 1. Planar multilayer structure for thermal modeling with perfusion

Due to the symmetry of heat transfer, the thermal model with perfusion (based on Pennes model [1,7]) in time domain can be reduced to 1D case for each layer and it takes the form:

$$k_i \frac{\partial^2 T(x,t)}{\partial x^2} - c_{vi} \frac{\partial T(x,t)}{\partial t} = -q_{vi} - w_i \rho_b c_b [T_b - T(x,t)] \quad (1)$$

Applying Laplace transform for $s=j\omega$, one can rewrite eqn. (1):

$$L_i^2(j\omega) \frac{\partial^2 T(j\omega)}{\partial x^2} - T(j\omega) = -\frac{L_i^2(j\omega)}{k_i} q_{vpi} \quad (2)$$

where power density q_{vpi} and diffusion length L_i are expressed as:

$$q_{vpi} = q_{vi} + w_i \rho_b c_b T_b \quad (3)$$

$$L_i(j\omega) = \sqrt{\frac{k_i}{j\omega c_{vi} + w_i \rho_b c_b}} \quad (4)$$

Analytical solution of (2) in frequency domain for i -th layer can be presented as:

$$T(x, j\omega) = A_i e^{-\frac{x}{L_i}} + B_i e^{\frac{x}{L_i}} + \frac{L_i^2}{k_i} q_{vpi} \quad (5)$$

In order to get the final solution, the boundary conditions have to be defined as in eqs. (6-9).

Temperature continuity at interfaces between the layers.

$$T_i(x) = T_{i+1}(x) \quad (6)$$

Flux continuity at the front surface (convective cooling).

$$-k_1 \frac{dT_1(0)}{dx} + h_0 T_1(0) = q_0 \quad (7)$$

Flux continuity at the interface between the layers.

$$-k_i \frac{dT_i(x_i)}{dx} + q_i = -k_{i+1} \frac{dT_{i+1}(x_i)}{dx} \quad (8)$$

Flux continuity at the bottom surface.

$$-k_n \frac{dT_n(x_n)}{dx} + q_n = h_n T_n(x_n) \quad (9)$$

Boundary conditions lead to formulate the set of linear equations with unknown integration constants A_i, B_i .

$$Q \cdot [AB] = P \quad (10)$$

where Q is a $(2n \times 2n)$ transform matrix, $[AB]$ is the column $(2n \times 1)$ of integration constants, and P is the column of power excitations $(2n \times 1)$. Once we know the integration constants $[AB] = Q^{-1}P$, temperature in each layer can be easily calculated.

Finally, thermal impedance graphically represented by the Nyquist plot takes the form:

$$Z_{th}(x, j\omega) = \frac{T(x, j\omega)}{P(j\omega)} \quad (11)$$

where $P(t) = P_0 \delta(t)$ is the total power dissipated in the structure.

$$P_0 = \sum_{i=1}^n (q_{vpi} d_i + q_i) S \quad (12)$$

where S is the cross-sectional surface of the object perpendicular to Ox axis.

Table 1 shows values of thermal parameters of an exemplary tissue structure used for simulations [19].

Tab. 1. Values of parameters of a skin tissue for thermal modeling [19]

$k_i, \text{W/m}\cdot\text{K}$	d_i, m	$w_i, 1/\text{s}$	$c_{thi}, \text{J/Km}^3$
0.24	0.0008	0	4308000
0.45	0.001	0.00125	3960000
0.19	0.003	0.00125	3960000

3. Cylindrical-symmetry n-layer thermal model with perfusion

The cylindrical multilayer model (Fig. 2) is similarly defined as the planar one mentioned above. Obviously, there is no convection cooling in the first inner layer of the structure.

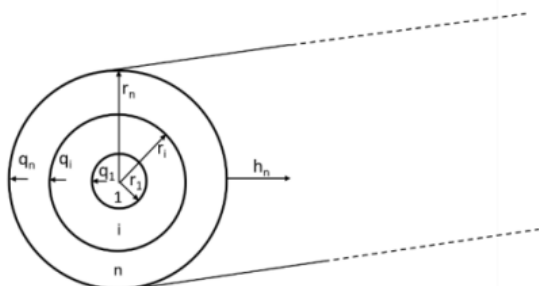


Fig. 2. Cylindrical multilayer structure for thermal modeling with perfusion

Due to the cylindrical symmetry, 3D model can be reduced to 1D one expressed in the cylindrical coordinates:

$$k_i \nabla^2 T_i(r, j\omega) - j\omega c_{vi} T_i(r, j\omega) = -\{q_{vi} + w_i \rho_b c_b [T_b - T(r, j\omega)]\} \quad (13)$$

The general solution of (13) is:

$$T_i(r) = A_i I_0\left(\frac{r}{L_i}\right) + B_i K_0\left(\frac{r}{L_i}\right) + \frac{L_i^2(j\omega)}{k_i} q_{vpi} \quad (14)$$

One should notice that for the first layer eq. (14) is expressed as:

$$T_1(r) = A_1 I_0\left(\frac{r}{L_1}\right) + \frac{L_1^2(j\omega)}{k_1} q_{vp1} \quad (14)$$

As before, the boundary conditions have to be defined. Temperature continuity at the interface between the layers.

$$T_i(r_i) = T_{i+1}(r_i) \quad (16)$$

Flux continuity at the interface between the layers.

$$-k_i \frac{dT_i(r_i)}{dr} + q_i = -k_{i+1} \frac{dT_{i+1}(r_i)}{dr} \quad (17)$$

Flux continuity with convection at the outer surface.

$$-k_n \frac{dT_n(r_n)}{dr} = q_n + h_n T_n(r_n) \quad (18)$$

Cylindrical structure can model a vessel in the tissue. The first layer contains blood, the second one refers to a blood vessel wall and the last one corresponds to muscles. Typical values of thermal parameters are in Table 2 [19].

Tab. 2. Values of parameters of a vessel surrounded by muscles [19]

$k_i, \text{W/m}\cdot\text{K}$	d_i, m	$w_i, 1/\text{s}$	$c_{thi}, \text{J/Km}^3$
0.52	0.002	0.05...0.00125	3797850
0.46	0.0022	0.00125	3643212
0.49	0.005	0.00125	3728890

4. $R_{th}C_{th}$ Foster network approximation

The models presented above generates thermal impedance $Z_{th}(j\omega)$ in frequency domain. In order to determine the temperature vs. time $T(t)$ as a response for any possible excitation, N -order Foster network approximation is used.

$$Z_{th}(s) = \sum_{i=1}^N \frac{R_i}{1+s\tau_i} \quad (20)$$

At first, in order to get the Foster approximation of thermal multilayer structure, the VF method is used [14,15]. It allows estimating the poles of (20) using LSM . VF ensures the high convergence of numerical estimation of poles distribution. The thermal resistances R_i in (20) are also calculated using LSM as one can formulate the linear set of equations where R_i are the unknown variables.

Having thermal time constants distribution (the Foster network) $R_i(\tau_i)$, for $i=1,2,\dots,N$, the impulse temperature response $h(t)$ of a thermal structure can be defined.

$$h(t) = \sum_{i=1}^N R_i e^{-\frac{t}{\tau_i}} \quad (21)$$

At last, temperature $T(t)$ can be calculated for any given power $P(t)$.

$$T(t) = h(t) * P(t) \quad (22)$$

where $*$ denotes the convolution.

5. Program for simulation biomedical structures

The program *FTOI_models* (*Frequency domain Thermal Object Identification*) implementing different kind of thermal models were written in Matlab environment. It shows the structure of each model and the set of parameters. Model's parameters have default values but can be changed by the user.

The number of model's layers and time constants for Foster network can be defined independently. The Nyquist plot of thermal impedance is the main result of the heat transfer model. Next, $R_{th}C_{th}$ Foster network approximation is calculated using *VF* method. In order to get the satisfactory results, the user can define frequency range and number of discrete frequency points for inverse problem solution using *VF*. Program can create a few graphical diagrams: Nyquist plots of thermal impedance and its approximation by Foster network, discrete time constant distribution and temperature evolution in time for different excitations. Fig. 3 presents the entrance window of *FTOI_models* program.

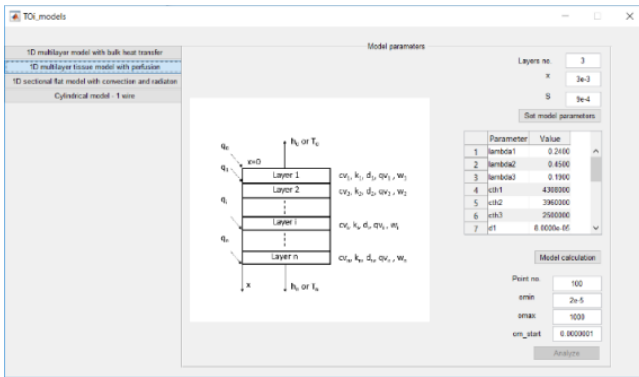


Fig. 3. Main window of the *FTOI_models* simulation program

6. Examples of the simulation results

Planar model

Two exemplary simulations were performed. At first, the influence of perfusion was investigated for a planar multilayer structure – Table 3. The model parameters are in Table 1. These parameters are very typical for a skin tissue. The similar simulations confirmed the impact of natural convection on the upper surface of the structure on thermal time constants distribution $R(\tau)$ – Table 4.

Tab. 3. Differences of thermal time constants for 3-layer planar model for $x=0$, with and without perfusion

With perfusion			
$R_i, K/W$	0.33	1.12	15.04
τ_i, s	3.85	13.85	144.70
Without perfusion, $w_1=w_2=w_3=0$			
$R_i, K/W$	0.44	1.60	19.01
τ_i, s	3.85	14.00	163.74

Tab. 4. Differences of thermal time constants for 3-layer planar model with perfusion for different convection on upper surface

$h_0 = 15 W/m^2K$			
$R_i, K/W$	0.33	1.12	13.14
τ_i, s	3.81	13.69	130.95
$h_0 = 30 W/m^2K$			
$R_i, K/W$	0.33	1.11	10.26
τ_i, s	3.71	13.36	110.13

One can see that the highest time constant strongly depends on heat transfer coefficient h_0 . The higher the convection, the lower the time constant τ_3 . Fig. 4 exhibits the thermal characteristics of the 3-layer planar structure: thermal impedance (Nyquist plot), discrete thermal time constant distribution and step-function temperature response.

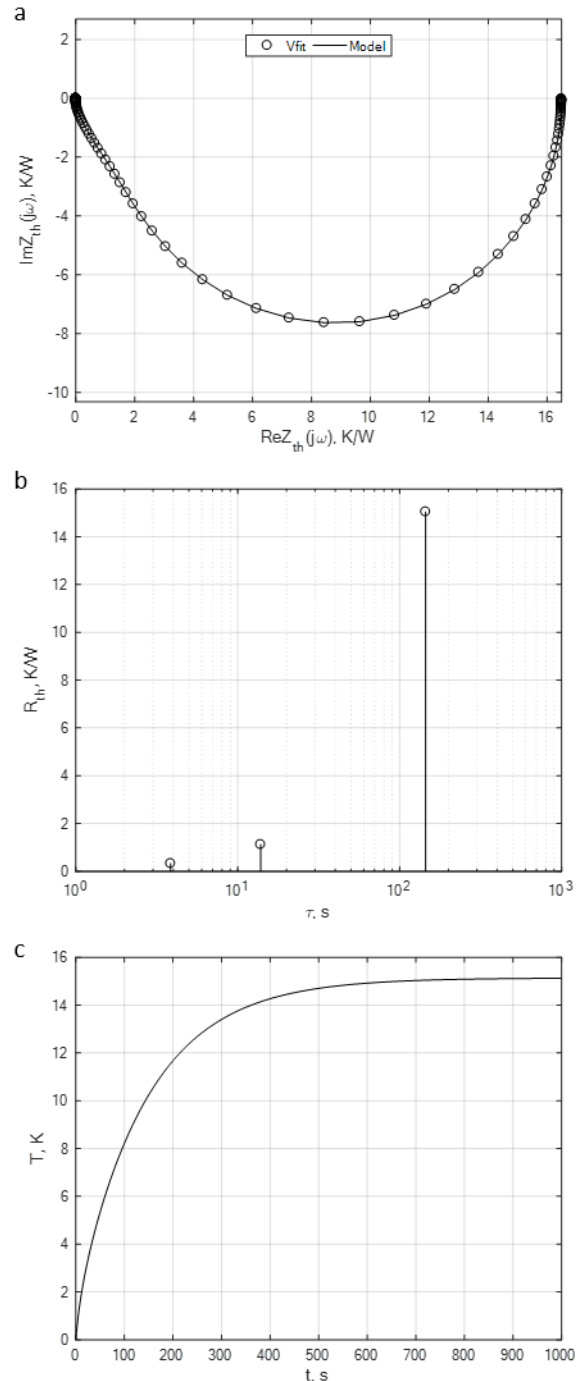


Fig. 4. Thermal impedance $Z_{th}(j\omega)$. a) Thermal time constants distribution $R(\tau)$, b) Temperature response on upper layer, c) for 3-layer planar model for $x=0$ mm, with perfusion, area of tissue $S=9 cm^2$, power dissipated in the upper layer (model's parameters in Table 1), $h_0=8 W/m^2K$ $h_n=100 W/m^2K$

Cylindrical model

A cylindrical multilayer structure simulates a vessel. The highest value of perfusion is for the first inner layer. Fig. 5 exhibits the thermal characteristics of the modeled structure. In Table 5 simulation results for different values of perfusion (0.01 -0.05) 1/s are presented.

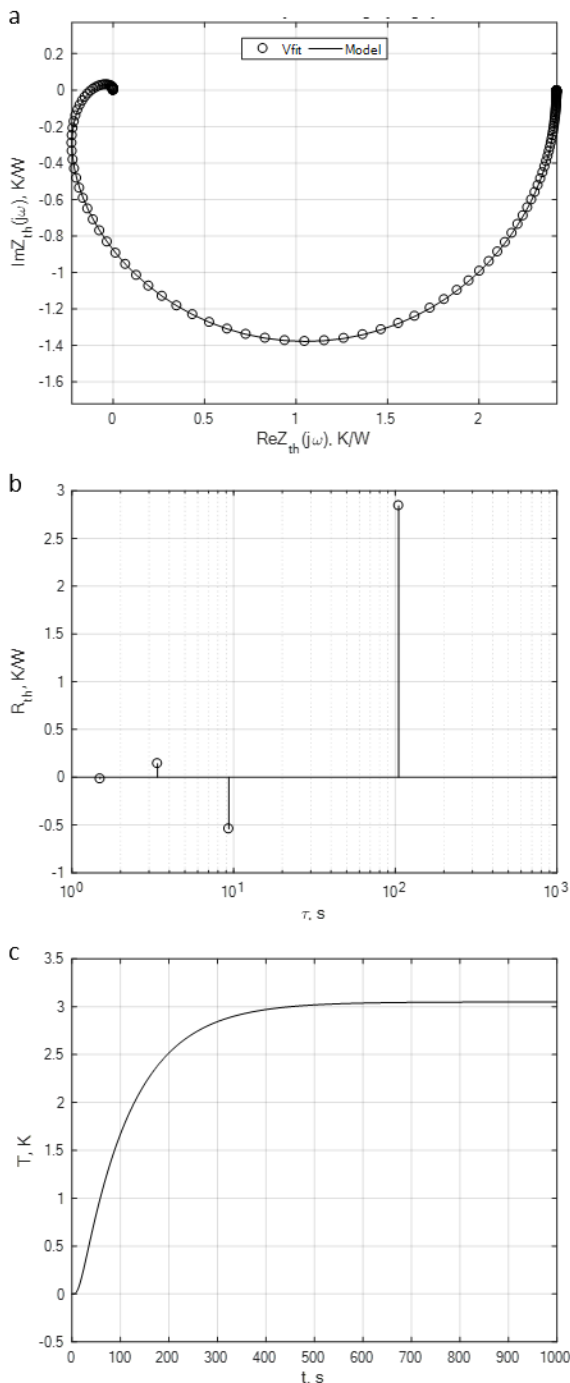


Fig. 5. Thermal impedance $Z_{th}(j\omega)$. a) Thermal time constants distribution $R(\tau)$, b) Temperature response on upper layer, c) for 3-layer cylindrical model for $r=5$ mm, with perfusion, length of the structure $L=10$ cm, power dissipated in the first inner layer, perfusion $w_1=0.05$ 1/s, $h_n=20$ W/m²K

Tab. 5. Differences of thermal time constants for 3-layer cylindrical model with different perfusion

$w_1 = 0.05$ 1/s				
R_i , K/W	-0.017	0.14	-0.54	2.84
τ_i , s	1.50	3.38	9.35	105.04
$w_1 = 0.01$ 1/s				
R_i , K/W	-0.0129	0.1321	-0.7114	6.8444
τ_i , s	1.3924	3.5911	11.7500	210.3794

The negative values of amplitudes of time constants are necessary to model transfer impedance where temperature is measured far away from the heat source. It is impossible to get

a delay in temperature evolution in time having the positive amplitudes of time constants only.

7. Conclusions

Heat transfer modeling combined with Foster network approximation of biological multilayer structures seems to be an effective tool for inverse thermal problem investigations. In practice after measurement the temperature evolution in time, we use optimization to identify the parameters of the model. This process is ill-conditioned in general case. Therefore the modeling and $R_{th}C_{rh}$ Foster network approximation could be an initial stage of the research. Knowing the expected values of the model's parameters can be helpful for more precise inverse thermal problem solutions.

For such a scenario of investigations of bioheat transfer we propose semi-analytical modeling in frequency domain which is fast and accurate enough for multilayer structures with additional assumption of their symmetry. Simulation program of heat transfer in multilayer structures was prepared in Matlab environment and chosen examples were presented. The program will be upgraded by new models soon.

8. References

- [1] <https://nl.mathworks.com/help/ident/ref/tfest.html>
- [2] <https://www.comsol.com>
- [3] <https://www.ansys.com/>
- [4] Chatzipanagiotou P., Strąkowska M., De Mey G., Chatziathanasiou V., Więcek B.: A new software tool for transient thermal analysis based on fast IR camera temperature measurement. Measurement Automation Monitoring, Feb. 2017, no. 62, vol. 63, ISSN 2450-2855, pp. 49-51.
- [5] Strakowska M., Strąkowski R., Strzelecki M., De Mey G., Więcek B.: Thermal modelling and screening method for skin pathologies using active thermography. Biocybernetics and Biomedical Engineering, 10.1016/j.bbe.2018.03.009.
- [6] Strakowska M., Chatzipanagiotou P., De Mey G., Chatziathanasiou V., Więcek B.: Novel software for medical and technical Thermal Object Identification (TOI) using dynamic temperature measurements by fast IR cameras. 14th Quantitative InfraRed Thermography Conference, QIRT 2018, June 25-29, 2018, Berlin, DOI: 10.21611/qirt.2018.053 <http://qirt.gel.ulaval.ca/archives/qirt2018/papers/053.pdf>
- [7] Strakowska M., Więcek B., Strzelecki M., Kaszuba A.: Screening procedure based on cold provocation and thermal tissue modeling. 13th Quantitative Infrared Thermography Conference, 04-08 July 2016, Gdansk, Poland.
- [8] Strąkowska M., Strąkowski R., Strzelecki M., De Mey G., Więcek B.: Evaluation of Perfusion and Thermal Parameters of Skin Tissue Using Cold Provocation and Thermographic Measurements, Metrology and Measurement Systems. The Journal of Committee on Metrology and Scientific Instrumentation of Polish Academy of Sciences, Volume 23, Issue 3 (Sep 2016).
- [9] Strakowska M., De Mey G., Więcek B., Strzelecki M.: A Three Layer Model for The Thermal Impedance of The Human Skin: Modeling And Experimental Measurements. Journal of Mechanics in Medicine and Biology, 15(3), 2015, DOI: 10.1142/S021951941550044X.
- [10] Szekely V.: Identification of RC networks by deconvolution: Chances and limits. IEEE Trans. Circuits Syst., vol. 45, no. 3, pp. 244-258, 1998.
- [11] Marco S., Palcin J., Samitier J.: Improved multiexponential transient spectroscopy by iterative deconvolution. IEEE Trans. In Instrumentation and Measurement, vol. 50, pp. 774-780, 2001.
- [12] Garnier, H., Mensler M., Richard A.: Continuous-time Model Identification from Sampled Data: Implementation Issues and Performance Evaluation. International Journal of Control, 2003, Vol. 76, Issue 13, pp. 1337-1357.
- [13] Ljung, L.: Experiments With Identification of Continuous-Time Models. Proceedings of the 15th IFAC Symposium on System Identification. 2009.

- [14] Gustavsen B, Semlyen A.: Rational approximation of frequency domain responses by vector fitting, IEEE Trans. Power Delivery, vol. 14, no. 3, pp. 1052–1061, Aug. 1999.
- [15] Gustavsen B.: Improving the pole relocating properties of vector fitting, IEEE Trans. Power Delivery, vol. 21, no. 3, pp. 1587–1592, Aug. 2006.
- [16] Górecki K., Rogalska M., Zarębski J.: Parameter estimation of the electrothermal model of the ferromagnetic core. Microelectronics Reliability, Vol. 54, No. 5, pp. 978-984, 2014.
- [17] Jibia A.U., Salami M-J: An Appraisal of Gardner Transform-Based Method of Transient Multiexponential Signal Analysis. International Journal of Computer theory and Engineering, vol.4, pp. 16-24, 2012.
- [18] T3Ster-Master Thermal Evaluation Tool – User’s Manual Version 2.2, Mentor Graphics Corporation.
- [19] Hartevelde A. A., Denswil N. P., Van Hecke W., Kuijf H. J., Vink A., Spliet W. G. M., Daemen M. J., Luijten P. R., Zwanenburg J. J.M., Hendrikse J., van der Kolk A. G.: Data on vessel wall thickness measurements of intracranial arteries derived from human circle of Willis specimens. Data in Brief, Vol. 19, August 2018, pp. 6-12.

Received: 12.12.2018

Paper reviewed

Accepted: 04.02.2019

Maria STRĄKOWSKA, PhD

Maria Strąkowska received the MSc degree in electronics in 2010 and the PhD degree in informatics in 2017, both from Lodz University of Technology (LUT). From 2017 she is employed at the Institute of Electronics LUT as Associate Professor. Her scientific interests are focused on computer modeling of heat transfer phenomena in medicine (human tissue) and also electronics Her field of interest are also thermographic image processing and thermovision measurements.

e-mail: maria.strakowska@p.lodz.pl



Prof. Bogusław WIĘCEK

Prof. Bogusław Więcek is the head of the Electronic Circuits and Thermography Department at the Institute of Electronics, Lodz University of Technology. He specializes in computer thermography and modelling thermal effects in electronic devices and circuits. He is a member of the scientific committee of the international Quantitative Infrared Thermography Conference and the chairmen of the Thermography and Thermometry in Infrared Conference.

e-mail: boguslaw.wiecek@p.lodz.pl

